



Fully embedded CuNWs/PDMS conductor with high oxidation resistance and high conductivity for stretchable electronics

Bowen Zhang^{1,2} , Wanli Li^{1,2} , Yang Yang³ , Chuantong Chen² , Cai-Fu Li^{2,*} , and Katsuaki Suganuma^{2,*} 

¹Department of Adaptive Machine Systems, Graduate School of Engineering, Osaka University, Osaka, Japan

²The Institute of Scientific and Industrial Research (ISIR), Osaka University, Osaka, Japan

³Pacific Northwest National Laboratory, 999, Richland, WA 99352, USA

Received: 7 November 2018

Accepted: 4 January 2019

Published online:

14 January 2019

© Springer Science+Business Media, LLC, part of Springer Nature 2019

ABSTRACT

In typical CuNWs-based conductors, CuNWs are deposited on or semi-embedded in the surface of substrates, which cannot avoid the oxidation. Here, we report a strategy to fabricate highly conductive and stretchable conductor with enhanced reliability and robustness through fully embedding CuNWs into the surface layer of poly(dimethylsiloxane) (PDMS) and followed with a high-intensity pulsed light technique. The light energy absorbed by the film not only removes the oxides on the surface of nanowires but also enhances the inter-nanowire connection to achieve high conductivity. The fully embedded CuNWs/PDMS structure showed excellent oxidation resistance in high-humidity and high-temperature environments (85 °C, 85% RH), and maintained a low sheet resistance when subjected to 30% of strain for 1000 cycles. Stretchable dipole antenna was fabricated using the fully embedded CuNWs/PDMS conductors, which retained its sensitivity to specific radio frequencies even after 500 cycles of the stretching/releasing process. Furthermore, a stretchable conductive heater was demonstrated, verifying the applicability of our fully embedded conductor for wearable electronics. We believe this work might open up new opportunities for the wide range of practical applications of CuNW-based conductors.

Introduction

Stretchable and flexible electronic devices have garnered increasing attention due to their softness, lightweight, portability and low-cost processing

[1, 2]. They have been applied in various wearable and mobile devices for real-time healthcare monitoring and human daily life management [3–5]. Consequently, substantial progress has been made in designing stretchable conductors with diverse

Address correspondence to E-mail: cfi0619@gmail.com; suganuma@sanken.osaka-u.ac.jp

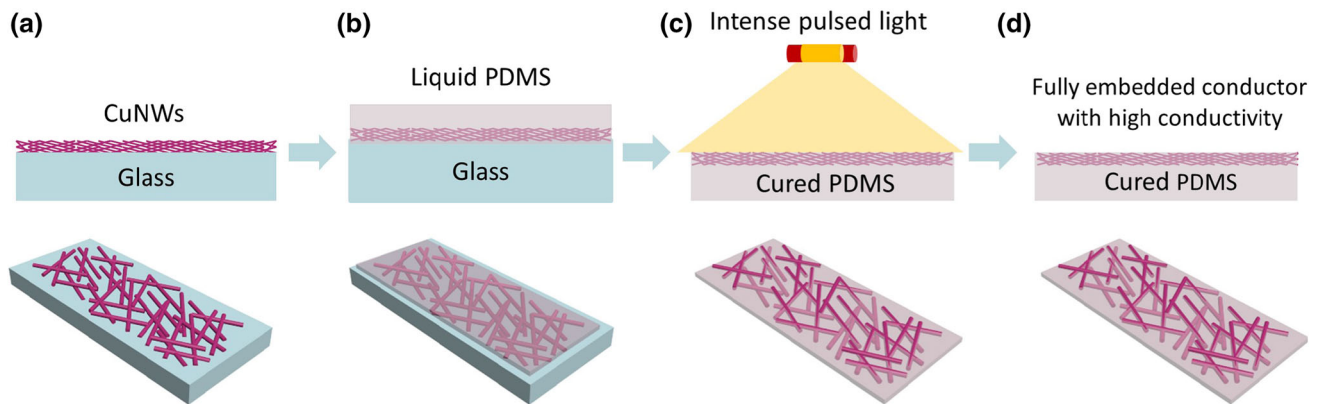


Figure 1 The cross-sectional and over view showing the fabrication process of fully embedded CuNWs/PDMS conductors.

materials, such as graphene [6], carbon nanotubes, [7] silver nanowires (AgNWs) [8], copper nanowires (CuNWs) [9], nanopatterned metallic films [10], conductive polymers [11] and hybrid materials [12]. Among these, metallic nanowires have attracted considerable attention because they can be cost effectively processed by coating a nanowire solution on a substrate [13, 14]. In this case, silver has been so far the most explored metal for the fabrication of metallic nanowires [15, 16]. Recently, substitution of silver by copper would be of great interest mainly because the electrical conductivity of copper ($5.96 \times 10^7 \text{ S m}^{-1}$) is comparable to that of silver ($6.3 \times 10^7 \text{ S m}^{-1}$) [17, 18], while the cost is a 100 times less expensive than silver [9, 14, 19].

However, the poor stability of copper against oxidation in ambient conditions largely overshadows their practical applications [20–22]. Lately, several demonstrations have shown progress in improving the performance of CuNWs-based conductor, including sheet resistance, flexibility and stretchable properties [23, 24]. Hu et al. [25] demonstrated that the chemical pre-treatment of CuNWs network with 6-aminohexanoic acid could improve the stretchability of the conductor. High stretchability was obtained in a wide range of strain rates over 200 cycles of stretching. Cheng et al. [14] succeeded in partially embedding the CuNWs network in the polymer matrix through a fabrication and transfer technique. The conductor exhibited improved mechanical robustness against bending and stretching tests. The sheet resistance increased about 4 times after cycling between 0 and 10% strain at 20 cycles. Ding et al. [26] fabricated partially embedded CuNWs/polyurethane (PU) conductor using a one-step photonic

sintering technique, with a sheet resistance of $22.1 \Omega/\text{sq}$ and transmittance of 78%. The resistance of the conductor increased about 3 times after 1000 cycles of stretching/releasing under 10% strain. However, in these CuNWs-based conductors, CuNWs are deposited on or semi-embedded in the surface layer of substrates, which cannot avoid the oxidation. Additionally, CuNWs are easily delaminated from the substrates under repeated mechanical loading. Therefore, a fast and powerful method is urgently required to fabricate CuNWs-based conductors with high conductivity, high stretchability and high reliability simultaneously.

In this paper, a fully embedded conductor with CuNWs embedded in the surface layer of poly(dimethylsiloxane) (PDMS) was successfully achieved, which possess outstanding oxidation resistance as well as high conductivity. The cross-sectional and over view fabrication process is schematically illustrated in Fig. 1. During the fabrication process, the curing conditions of PDMS and the accumulation of PDMS at CuNWs junctions lead to the sharp increase in resistance and then limit the application of CuNWs/PDMS conductor. Therefore, a high speed and room temperature operated high-intensity pulsed light technique was innovatively introduced to remove the oxides on the surface of CuNWs and enhance the connection between CuNWs at the same time. The influence of light parameters on the conductivity of fully embedded CuNWs/PDMS conductors was systematically investigated. After that, the stretchability and oxidation resistance of such conductors were investigated in detail. After 1000 stretching/releasing cycles at 30% strain, the resistance of the fully embedded

conductor increased less than 3 times compared with about 800 times of the semi-embedded conductor. In the latter stages, a stretchable conductive heater and a stretchable antenna are demonstrated by using the fully embedded CuNWs/PDMS conductors. The antenna could retain its sensitivity to specific radio frequencies even after 500 cycles of the stretching/releasing process.

Materials and methods

Synthesis of CuNWs

Anhydrous copper dichloride (CuCl_2 , 95%), glucose (98%), octadecylamine (ODA), chloroform and isopropanol were purchased from Wako Chemicals. All reagents were analytical grade and were used without further purification.

The synthesis of CuNWs involves a Cu(II) salt, a surfactant and a reducing agent, using water as the solvent. In a typical procedure, 0.4 mmol CuCl_2 , 0.4 mmol glucose and 2.4 mmol ODA were mixed in 30 mL of water at room temperature for 2 h under magnetic stirring until the solution gradually became a blue emulsion. Then, the feedstock was transferred into a 50-mL capacity Teflon-lined autoclave and heated at 120 °C for 24 h. When the autoclave was cooled to room temperature naturally, the reddish product was collected by centrifugation, washed 3 times with water, chloroform and isopropanol (IPA), respectively. Finally, the CuNWs were dispersed in IPA to make CuNWs ink for further use.

Fabrication of conductors by spray coating and photonic sintering technique

Firstly, the as-prepared CuNWs were diluted to the desired concentration about 20 mmol/L and then subjected to ultrasonic vibration to ensure a homogeneous distribution. Glass substrate was placed on a hot plate with a temperature of 40 °C, which could effectively negate the aggregation of CuNWs due to the rapid evaporation of IPA on the hot plate. Liquid PDMS was prepared by mixing the “base” and the “curing agent” at a ratio of 10:1, followed by a vacuum centrifuge process.

The fabrication process of fully embedded CuNWs/PDMS conductor is schematically illustrated in Fig. 1. For fully embedded structure, the

CuNWs ink was sprayed onto the glass substrates using a nozzle powered by an air compressor. After that, the liquid PDMS was cast onto the glass substrate which was coated with CuNWs film. Following that, all samples were thermally cured at 100 °C for 35 min and then peeled off from the glass substrate. This way, the CuNWs were fully embedded in the surface layer of PDMS. After that, the fully embedded CuNWs/PDMS films were treated with high-intensity pulsed light technique to obtain a conductive enhanced network. Finally, the CuNWs/PDMS conductors were carefully cut into thin strips ($5 \times 20 \text{ mm}^2$) for various evaluations.

Semi-embedding structured CuNWs/PDMS conductors were fabricated with the traditional method. Firstly, the liquid PDMS was cast onto a pre-cleaned glass substrate and peeled off after the same curing process. Then, the CuNWs ink was sprayed onto the surface of the cured PDMS, which also placed on a hot plate with the same temperature. After that, the sample was treated with high-intensity pulsed light technique under the same parameters and cut into the same thin strips.

Characterization

The morphologies of CuNWs, CuNWs/PDMS conductor were characterized by field-emission scanning electron microscopy (FESEM, Hitachi SU8020, Hitachi High Technologies) and transmission electron microscopy (TEM, JEM-ARM200F, JEOL Ltd). The cross section of CuNW was prepared by a focused ion beam (FIB, FB2100, Hitachi). The oxidation state of the sample was investigated by X-ray diffractometry (XRD, Rigaku Smart Lab, Rigaku). The electrical property of CuNWs/PDMS conductor was performed by attaching two ends of the sample onto a pair of grips in a dynamic mechanical analyzer (EZ Test, Shimadzu) with a speed of 60 mm/min. The resistance of printed electrodes during testing was recorded through a four-point probe method. The high-intensity pulsed light system used in this study was the Pulse Forge 3300 (Novacentrix, Austin, TX) that features a broadband emission range from 400 to 1500 nm. The water-cooled xenon lamp, located 10 mm from the substrate stage, can vary optical energy as a function of the electrical voltage and duration time. In this work, the duration time and electrical voltage was changed to supply optical energies ranging from 1.36 to 2.44 J/cm². The

environmental durability of the CuNWs/PDMS was evaluated at high temperatures of 85 °C with 85% relative humidity (85 °C–85% RH). The return losses of the V-shaped dipole antennas were evaluated inside an electromagnetic shielding bag at 0.5–3.5 GHz, using a network analyzer (E5061A; Agilent Technologies, Inc., USA).

Results and discussion

Figure 2a shows SEM images of the synthesized CuNWs. The average diameter of the nanowires was around 70 nm; the average length of the nanowires was around 70 μm , as calculated from 50 nanowires randomly selected from the SEM images. As seen from SEM images, these nanowires were uniform and well dispersed; no impurities (nanoparticles or other by-products) can be observed in the products. The magnified SEM image (Fig. 2a inset) reveals that the obtained nanowires exhibited a pentagon cross section. Figure 2b shows the surface of a single nanowire

using the high-resolution TEM (HRTEM) images. The distance of lattice spaces is 0.21 nm, which could be indexed to the {111} [27, 28] planes of metal Cu, which is consistent with previous reports [29–31]. Figure 2c shows the SEM image of the top surface of the fully embedded conductor. The CuNWs are bonded to the cured PDMS, and only scarce CuNWs are visible, all of the CuNWs being below the upper surface of PDMS. The cross section of the fully embedded conductor is shown in Figure S1, which further demonstrate the fully embedded structure. The SEM image of the semi-embedded conductor is shown in Fig. 2d. By high-intensity pulsed light process, some parts of the CuNWs were buried into the surface layer of PDMS and form the semi-embedded conductor. For our method, the fully embedded structure is formed during the curing process of PDMS, the main function of high-intensity pulsed light is to remove the oxide layer and improve conductivity. But for conventional methods, high-intensity pulsed light technique is mainly used to form semi-embedded structures.

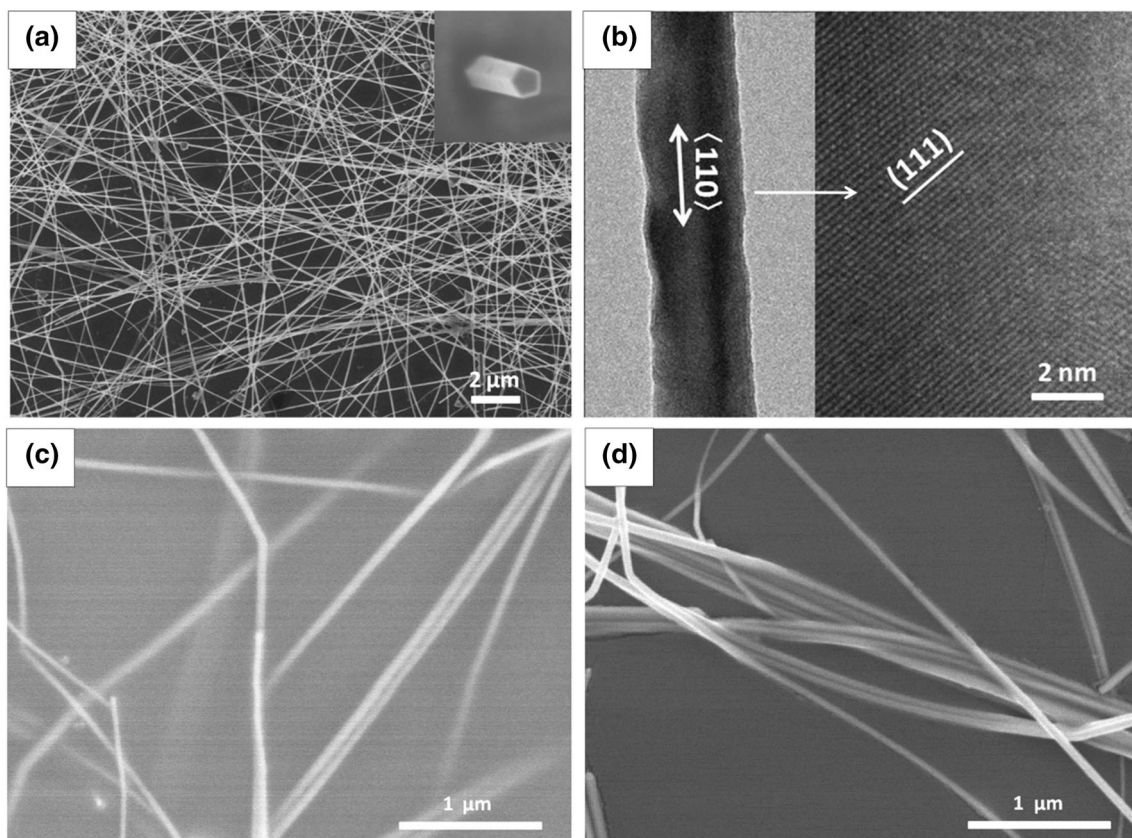


Figure 2 **a** SEM image of as-prepared CuNWs, inset is the cross section of a CuNW. **b** High-resolution TEM images of the CuNWs. SEM image of **c** fully embedded and **d** semi-embedded conductor.

The resistivity of CuNWs films was examined before and after casting the PDMS. The resistivity of CuNWs film is about 35 $\mu\Omega$ cm before the casting of PDMS. After casting PDMS, the sheet resistivity grows to 6319 $\mu\Omega$ cm and some of the samples even lose conductivity. Due to the low viscosity and surface energy of liquid PDMS, when it is poured onto the CuNWs film, the PDMS penetrates into the CuNWs network and accumulates at the CuNWs junctions, thus increasing the effective resistance of the sample [32]. At the same time, the high curing temperature of PDMS also accelerates the oxidation of CuNWs and leads to an increase in resistivity of CuNWs/PDMS conductors. In order to improve the conductivity of fully embedded conductor, the facile high-intensity pulsed light technique was introduced.

Figure 3a shows the resistivity evolution of fully embedded CuNWs/PDMS conductor after light treatment with different input energies of 1.36, 1.74, 2.15 and 2.44 J/cm², respectively. After the light treatment process, the resistivity of the sample is

significantly reduced from several thousand to tens $\mu\Omega$ cm. When the energy was as low as 1.36 J/cm², the resistivity of the fully embedded conductor after light treatment was around 94 $\mu\Omega$ cm. The resistivity was dramatically decreased to 31 $\mu\Omega$ cm and 20 $\mu\Omega$ cm when the energy was increased to 1.74 J/cm² and 2.15 J/cm², respectively. Unfortunately, increasing the energy to 2.44 J/cm² resulted in a higher resistivity around 40 $\mu\Omega$ cm. When the sample is treated with high light energy, the resistivity of the sintered electrodes begins to increase because the excessive energy during a short time may cause broke on the surface of CuNWs/PDMS conductor, and the CuNWs exposed to the surface of the PDMS was blown away and the transmittance of the sample had been increased. The stretching/releasing process of these four samples was also carried out as shown in Fig. 3a. The resistivity of all samples increased slightly after cycling test, which is mainly due to the composite structure of CuNWs and PDMS. It is worth noting that, the light treatment greatly

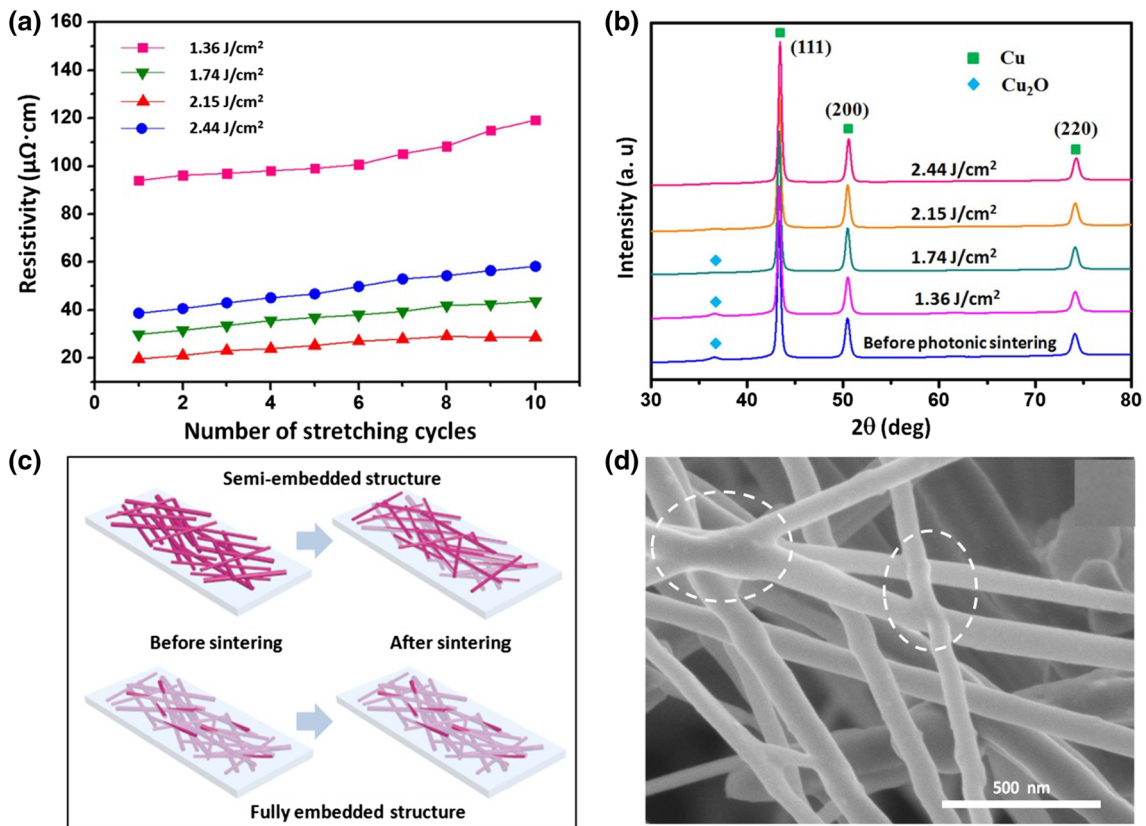


Figure 3 a Resistivity change of CuNWs/PDMS conductors during the stretching/releasing process. b XRD images of the CuNWs/PDMS conductor before and after high-intensity pulsed

light treatment. c The surface microstructure changes of the fully embedded structure and semi-embedded structure after the light treatment. d SEM image of the CuNWs after the light treatment.

enhanced the conductivity of the conductors, and the light energy of 2.15 J/cm^2 showed the best improvement, which was fixed in the follow-up experiment.

To explore the phase changes of CuNWs during the high-intensity pulsed light process, we examined the XRD results of the fully embedded conductor before and after the light treatment, which are shown in Fig. 3b. Before light treatment, we can see the peak at $2\theta = 36.4^\circ$, which corresponds to copper oxide (JCPDS 05-0667). [33] This indicates that high conductivity cannot be directly achieved in CuNWs/PDMS film. A weak Cu_2O peak was also observed in the samples that were treated with a low light energy of about 1.36 and 1.74 J/cm^2 . With the increase in light energy, the Cu_2O phase diminishes, leaving only the Cu phase, three diffraction signals can be readily indexed at $2\theta = 43.5^\circ$, 50.7° and 74.4° , which correspond to the (111), (200) and (220) crystal planes of face-centered-cubic copper (JCPDS 85-1326), respectively. There are no extra signals observed, indicating the high purity of copper and no other crystallites were observed in the product after light treatment. The reduction degree of the CuNWs showed good consistent with the resistivity change of the conductors. The reduction in the Cu_2O phase to pure Cu during flashlight sintering may be related to the photochemical reaction and the thermal reaction process in the presence of organics on the surface of CuNWs. During the growth of CuNWs, the capping agent ODA was gradually adsorbed on the surface of the newly emerging copper crystals and grew with the crystals to be a nanolayer on the surface of nanowire. It is believed that residual ODA may photodegrade to produce active H and N radicals under the irradiation of high-intensity light, which then reacted with Cu_2O to remove the oxidation layer [34].

The SEM images of the fully embedded and semi-embedded conductors before and after the high-intensity pulsed light treatment are shown in Figure S2. The corresponding schematic diagram is shown in Fig. 3c. It can be clearly seen that the morphology of the embedded structure before (Figure S2a) and after (Figure S2b) the light treatment has no obvious changes, which is mainly due to that most of the CuNWs are already embedded in the upper surface layer of the PDMS. For semi-embedded structure, the CuNWs are evenly distributed on the surface of PDMS before the light treatment, and no embedding

was observed (Figure S2c). After the light treatment, the CuNWs are partially embedded in the surface layer of PDMS (Figure S2d). The high-intensity pulsed light technique is a fast and powerful method to anneal metal nanostructure in the air without protective atmosphere [34]. And the main approach of light treatment is the thermal conversion of the metal or metal precursor into its conductive counterparts [35]. When the CuNWs/PDMS conductor is exposed to strong light, it absorbs very high light energy within microseconds. The energy absorbed by the conductor is converted to thermal energy, which sinters the CuNWs to produce high conductivity. At the same time, because of the high thermal conductivity of the CuNWs, the heat from the light is easily and rapidly transmitted from the upper wires to the lower wires along the film thickness [36, 37]. Hence, the upper wires catch the thermal energy first and form many more dots, and conductivity has been significantly improved as shown in Fig. 3d.

Based on these results, we can find that the high-intensity pulsed light plays an important role during the fabrication of fully embedded CuNWs/PDMS conductors. On the one hand, the oxide layer on the surface of CuNWs is removed. On the other hand, the distance between nanowires was reduced, and welding is formed between the nanowires. Both of which have greatly improved the conductivity of the CuNWs/PDMS conductors and laid the foundation for subsequent applications.

The stretchability of CuNWs/PDMS conductors after high-intensity pulsed light treatment was investigated. Figure 4a shows the resistance change of a CuNWs/PDMS conductor during the stretching process at a constant strain rate of 1 mm/min . The relative resistance of fully embedded conductor rose slowly at first. It increased to just 1.1 times when the strain was 20% and 2.5 times when the strain reached 50%. When the strain was further increased to 70% the resistance increased by about 8 times. At the same time, the resistance of semi-embedded conductor increased more than 20 times when the strain reached 70%. SEM image of the fully embedded conductor after stretching process is shown in Fig. 4b. As seen from the SEM image, the surface of the conductor formed into wrinkled structures without breaking after the stretching process. For fully embedded conductor, due to the existence of the PDMS matrix, the intrinsically loose CuNWs network was mechanically robust. In addition, the CuNWs are

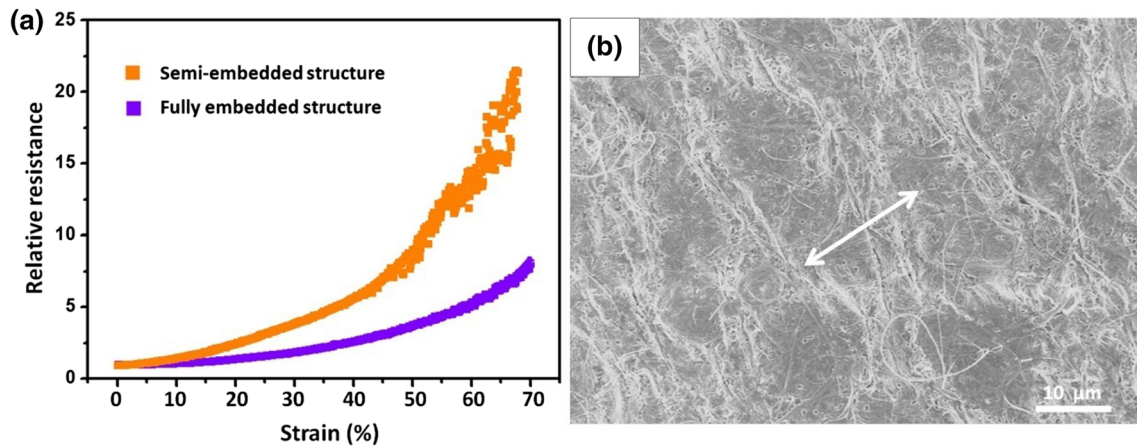


Figure 4 **a** Relative resistance (R/R_0) of fully embedded and semi-embedded CuNWs/PDMS conductors with strain up to 70% at a constant stretching speed of 1 mm/min. **b** SEM image of the CuNWs/PDMS conductor after stretching.

buried deeper than semi-embedded structure, so that the sample could maintain high electrical conductivity during the stretching process. For semi-embedded conductor, only some of the CuNWs were buried in the upper surface of PDMS; during the straining process, part of the contact spots among CuNWs became broken due to the sliding of nanowires under the stretching strain, and the concentration of CuNWs in certain areas was quickly reduced, all of which led to the large increase in resistance.

Dynamic stability is very important for a stretchable device. Therefore, the performance of the fabricated fully embedded and semi-embedded conductor was investigated over multiple stretch-relaxation cycles. Figure 5a, b shows the relative resistance of CuNWs/PDMS conductor measured during 1000 cycles, at a constant strain rate of 60 mm/min, with peak strain at 10, 20 and 30%, respectively. Figure 5a shows the resistance evolution of fully embedded conductor. The resistance increased to just 1.2 times upon being stretched to 10% strain. After repeatedly stretching/releasing under 20% strain, the resistance increased to 1.8 times. The resistance increased less than 3 times even after 1000 cycles under 30% strain, thus exhibiting an excellent stretching property compared with previous reports [38, 39]. For CuNWs/PDMS conductor with semi-embedded structure (Fig. 5b), resistance increased to 1.9 times upon being stretched to 10% strain. When stretched to 20% strain, the resistance increased to 7.0 times of original value. Under a 30% strain, after 400 cycles, the resistance increased to 16.0 times and further

increased near 800 times over 1000 cycles. During the stretching process, the weak contact spots in semi-embedded structure were easily broken, especially under 30% strain, and only a few locations transferred the electron and resulting in the low resistance. At the same time, the CuNWs network in fully embedded structure maintained stable contact spots, resulting in stable conductivity under a higher strain and improved dynamic stability. Combined with previous reports, it is clear that the superior dynamic stability of fully embedded conductor is mainly due to the outstanding stretchability of PDMS matrix, the strong adhesion between CuNWs and PDMS, and the buckled wavy shape of the CuNW/PDMS layer during the stretching process [14, 26]. These results clearly indicate that our fully embedded conductors represent an excellent advancement and can be successfully utilized in many stretchable devices.

The stability of our fully embedded CuNWs/PDMS conductors at high temperatures and high humidity is also required for its practical application. In order to confirm the antioxidation performance of CuNWs/PDMS conductors, we have compared the change of relative resistance for fully embedded and semi-embedded conductor with the temperature and relative humidity being 85 °C and 85%, respectively. The results are shown in Fig. 5c. For semi-embedded conductor, the relative resistance began to increase suddenly after just 1 h and rapidly increased to about 36 times after 12 h in high temperature and humidity. As a comparison, the relative resistance of fully embedded conductor remains almost stable, having only a slight increase of about 10 times after 12 h. In

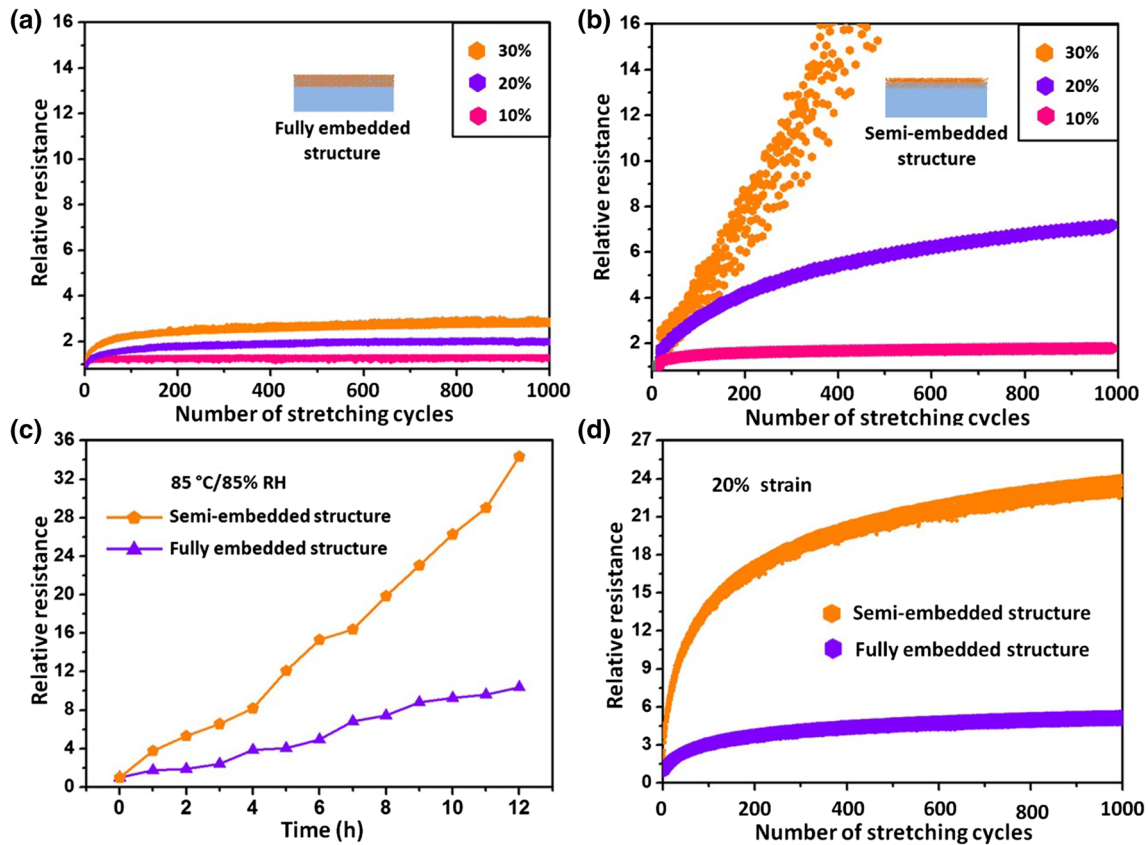


Figure 5 Performance comparison between semi-embedded and fully embedded CuNWs/PDMS structures. **a, b** Relative resistance of the conductors during the stretching/releasing process with the peak value of 10%, 20%, and 30% strain. **c** The change of relative

resistance in harsh environment (85 °C/85% RH). **d** After 85 °C/85% RH test, the relative resistance of conductors during the stretching/releasing process with the peak value of 20% strain.

addition, we have also compared the resistance evolution of two samples after 85 °C/85% RH test, with peak strain at 20%, during 1000 cycles. Figure 5d shows the dynamic stability of the two samples after 3 h under 85 °C/85% RH test. While under 20% strain, after 1000 cycles, the resistance increased about 6.0 times for embedding structure and over 24 times for non-embedding structure. For fully embedded conductor, PDMS substrate could effectively protect the CuNWs that were “underground” from the outer atmosphere. Therefore, it is easily understood they were stable as well. This result further indicates that the preferential oxidation of CuNWs can be significantly inhibited by the fully embedded structure.

The field of wireless communication devices requires technologies for the mass production of high-performance stretchable antennas [40, 41]. To demonstrate the applicability of our embedding structured CuNWs/PDMS conductors, V-shaped

dipole CuNWs antenna patterns were successfully fabricated. The antenna patterns were 30 mm in length and 5 mm in width with an angle of about 30°, and the sizes of the PDMS substrates were 30.0 mm × 30.0 mm as shown in Fig. 6a. Figure 6b shows the resonance frequency and the return loss of the CuNWs/PDMS antennas before and after 500-cycles stretching test, the stretching strain is 20%. As seen, the return loss of CuNWs/PDMS antennas before stretching test is around 22.6 dB, and after the stretching test it is 18.9 dB. There was no significant decrease in return loss of these two antennas, indicating that antenna sensitivity was maintained even after 500-cycles stretching test. Generally, the acceptable sensitivity for an antenna is that the return loss is less than 10 dB [42, 43]. Therefore, our results indicate that fully embedding structured CuNWs/PDMS antenna has high sensitivity and stability. The excellent stretching properties expand the application

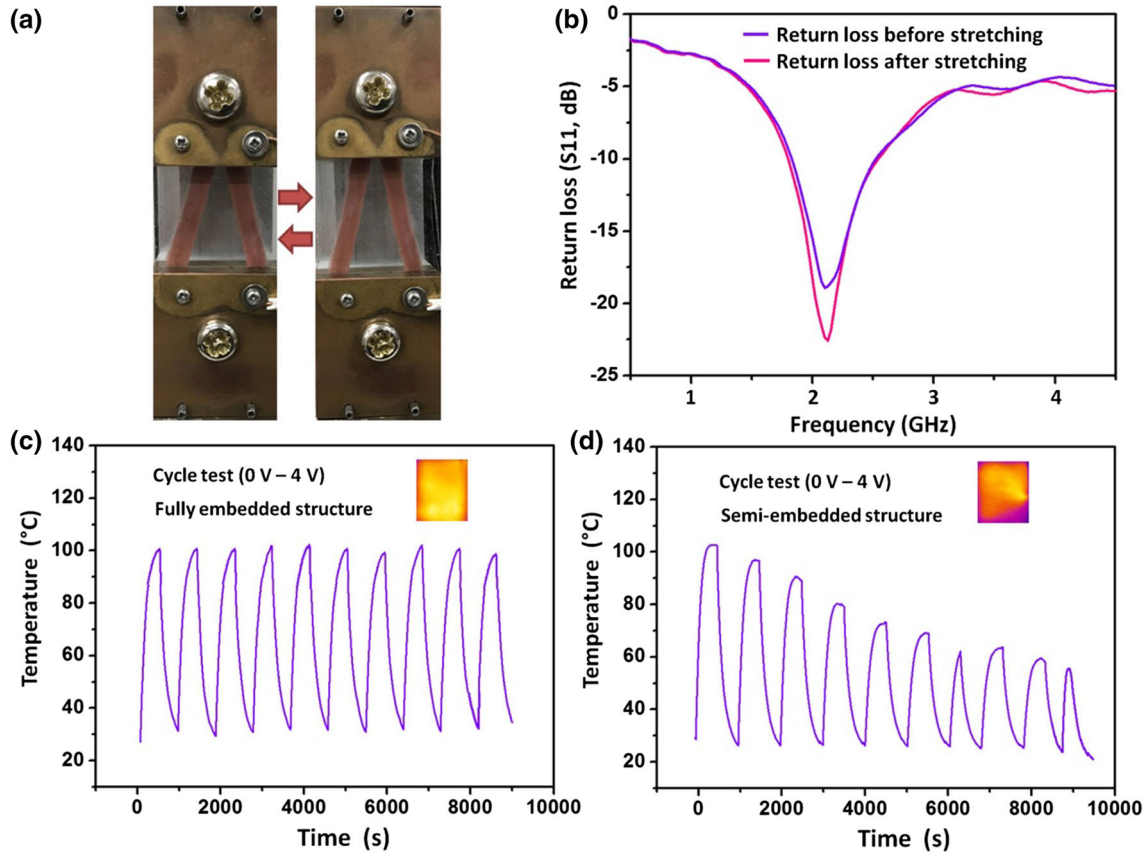


Figure 6 Applications of fabricated CuNWs/PDMS conductors for wearable electronics. **a** Optical images during the stretching process of CuNWs/PDMS antenna and **b** its return loss before and after the 500-cycles stretching test. The time-dependent average

temperature of the **c** semi-embedded and **d** fully embedded conductors at on/off responses over 10 cycles under an applied voltage of 4 V. The insets present infrared images of the conductor during repeated heating tests.

of embedding structured CuNWs/PDMS conductors into future wireless communication devices.

A stretchable conductive heater was fabricated as another emerging application to demonstrate the stability of CuNWs/PDMS conductor. A constant voltage was applied at both ends of the CuNWs/PDMS conductor to induce electrically driven resistive Joule heating. Figure 6c, d shows the time-dependent average temperature of the CuNWs/PDMS conductor at repeated applied voltages and temperature distribution infrared images. For fully embedded conductor, it was confirmed that there was no significant change in achievable temperature in repeated heating tests by inputting and turning off the voltage (4 V) for 10 times (Fig. 6c), and uniform heating can be seen throughout the entire conductor during this process. At the same time, the temperature response of semi-embedded conductor was decreased with the increase in time; the temperature distribution is uneven after 5 times heating test. The

stable temperature response of fully embedded conductor indicates that our fully embedded conductor can be feasible to applications such as automobile window defrosters that require fast temperature switching and stability.

Conclusions

In summary, CuNWs-based highly reliable, conductive and stretchable conductors were fabricated by embedding CuNWs below the surface layer of PDMS and completed with a simple high-intensity pulsed light process. The influence of light parameters on the performance of conductors was investigated. The light energy absorbed by the film not only removes the oxides on the surface of nanowires but also enhance the connection between nanowires to produce high conductivity. Due to the wrap of the CuNWs in the PDMS matrix, the fully embedded

conductor shows ultrahigh oxidation resistance, which remains stable in harsh environment of 85 °C and 85% RH. The electrical resistance of the conductor is maintained at low levels when the strain is more than 70%. The fully embedded conductor endured 1000 cycles of stretching/releasing at a rate of 60 mm/min, under 30% strain and showed a slight increase in resistance. Additionally, fully embedded conductor was used as a dipole antenna. The stretchable antenna retained its sensitivity to specific radio frequencies after 500 cycles of the stretching/releasing process. With their superior stability, conductivity and stretchability, the fabricated fully embedded CuNWs/PDMS conductors possess broad applications in stretchable strain sensors, skin sensors, bendable displays and wearable electronics.

Acknowledgements

B.Z. acknowledges the financial support from the China Scholarship Council for Ph.D. research (Grant 201706170023) at Osaka University. This work was also supported by Dynamic Alliance for Open Innovation Bridging Human, Environment and Materials from MEXT, Japan. The authors are thankful to the Comprehensive Analysis Center of Osaka University for TEM characterization and to T. Ishibashi for assistance with TEM.

Compliance with ethical standards

Conflicts of interest There are no conflicts to declare.

Electronic supplementary material: The online version of this article (<https://doi.org/10.1007/s10853-019-03333-x>) contains supplementary material, which is available to authorized users.

References

- [1] Hwang C, An J, Choi BD, Kim K, Jung SW, Baeg KJ, Kim MG, Kang MO, Hong J (2016) Controlled aqueous synthesis of ultra-long copper nanowires for stretchable transparent conducting electrode. *J Mater Chem C* 4:1441–1447
- [2] Yong HK, Sachse C, Machala ML, May C, Müller-Meskamp L, Leo K (2011) Photovoltaic devices: highly conductive PEDOT: PSS electrode with optimized solvent and thermal post-treatment for ITO-free organic solar cells. *Adv Func Mater* 21:1076–1081
- [3] Choi S, Lee H, Ghaffari R, Hyeon T, Kim DH (2016) Recent advances in flexible and stretchable bio-electronic devices integrated with nanomaterials. *Adv Mater* 28:4203–4218
- [4] Cheng T, Zhang Y, Lai WY, Huang W (2015) Stretchable thin-film electrodes for flexible electronics with high deformability and stretchability. *Adv Mater* 27:3349–3376
- [5] Lee H, Kim M, Kim I, Lee H (2016) Flexible and stretchable optoelectronic devices using silver nanowires and graphene. *Adv Mater* 28:4541–4548
- [6] Tassin P, Koschny T, Kafesaki M, Soukoulis CM (2012) A comparison of graphene, superconductors and metals as conductors for metamaterials and plasmonics. *Nat Photonics* 6:259–264
- [7] Kobylko M, Kociak M, Sato Y, Urita K, Bonnot AM, Kasumov A, Kasumov Y, Suenaga K, Colliex C (2014) Ballistic- and quantum-conductor carbon nanotubes: a reference experiment put to the test. *Phys Rev B* 90(19):195431
- [8] Moon H, Won P, Lee J, Ko SH (2016) Low-haze, annealing-free, very long Ag nanowire synthesis and its application in a flexible transparent touch panel. *Nanotechnology* 27:295201
- [9] Zhang D, Wang R, Wen M, Weng D, Cui X, Sun J, Li H, Lu Y (2012) Synthesis of ultralong copper nanowires for high-performance transparent electrodes. *J Am Chem Soc* 134:14283–14286
- [10] Catrysse PB, Fan S (2010) Nanopatterned metallic films for use as transparent conductive electrodes in optoelectronic devices. *Nano Lett* 10:2944–2949
- [11] Abidian MR, Kim DH, Martin DC (2006) Conducting-polymer nanotubes for controlled drug release. *Adv Mater* 18:405–409
- [12] Nguyen DD, Tai NH, Chen SY, Chueh YL (2012) Controlled growth of carbon nanotube-graphene hybrid materials for flexible and transparent conductors and electron field emitters. *Nanoscale* 4:632–638
- [13] Won Y, Kim A, Yang W, Jeong S, Moon J (2014) Annealing-free fabrication of highly oxidation-resistive copper nanowire composite conductors for photovoltaics open. *NPG Asia Mater* 6:e105
- [14] Cheng Y, Wang S, Wang R, Sun J, Gao L (2014) Copper nanowire based transparent conductive films with high stability and superior stretchability. *J Mater Chem C* 2:5309–5316
- [15] Yang Y, Ding S, Araki T, Jiu J, Sugahara T, Wang J, Vanfleteren J, Sekitani T, Sugauma K (2016) Facile fabrication of stretchable Ag nanowire/polyurethane electrodes using high intensity pulsed light. *Nano Res* 9:401–414
- [16] Yang Y, Xu K, Vervust T, Vanfleteren J (2018) Multifunctional and miniaturized flexible sensor patch: design and

- application for in situ monitoring of epoxy polymerization. *Sens Actuators B Chem* 261:144–152
- [17] Mallikarjuna K, Hwang HJ, Chung WH, Kim HS (2016) Photonic welding of ultra-long copper nanowire network for flexible transparent electrodes using white flash light sintering. *RSC Adv* 6:4770–4779
- [18] Hatami M (2017) Production and morphological characterization of low resistance polyimide/silver nanowire nanocomposites: potential application in nanoconductive adhesives. *J Mater Sci Mater Electron* 28(4):3897–3908
- [19] Rathmell AR, Bergin SM, Hua YL, Li ZY, Wiley BJ (2010) The growth mechanism of copper nanowires and their properties in flexible, transparent conducting films. *Adv Mater* 22:3558–3563
- [20] Dou L, Cui F, Yu Y, Khanarian G, Eaton SW, Yang Q, Resasco J, Schildknecht C, Schierle-Armdt K, Yang P (2016) Solution-processed copper/reduced-graphene-oxide core/shell nanowire transparent conductors. *ACS Nano* 10:2600–2606
- [21] Hsu PC, Wu H, Carney TJ, McDowell MT, Yang Y, Garnett EC, Li M, Hu L, Cui Y (2012) Passivation coating on electrospun copper nanofibers for stable transparent electrodes. *ACS Nano* 6:5150–5156
- [22] Zeng D, Chen Y, Lu A, Li M, Guo H, Wang J, Peng DL (2013) Injection synthesis of Ni–Cu@Au–Cu nanowires with tunable magnetic and plasmonic properties. *Chem Commun* 49:11545–11547
- [23] Guo H, Jin J, Chen Y, Liu X, Zeng D, Wang L, Peng DL (2016) Controllable synthesis of Cu–Ni core–shell nanoparticles and nanowires with tunable magnetic properties. *Chem Commun* 52:6918–6921
- [24] Niu Z, Fan C, Yi Y, Becknell N, Sun Y, Khanarian G, Kim D, Dou L, Dehestani A, Schierlearmdt K (2017) Ultrathin epitaxial Cu@Au core–shell nanowires for stable transparent conductors. *J Am Chem Soc* 139:7348–7354
- [25] Hu W, Wang R, Lu Y, Pei Q (2014) An elastomeric transparent composite electrode based on copper nanowires and polyurethane. *J Mater Chem C* 2:1298–1305
- [26] Ding S, Jiu J, Gao Y, Tian Y, Araki T, Sugahara T, Nagao S, Nogi M, Koga H, Sugauma K (2016) One-step fabrication of stretchable copper nanowire conductors by a fast photonic sintering technique and its application in wearable devices. *ACS Appl Mater Interfaces* 8:6190–6199
- [27] Han S, Hong S, Ham J, Yeo J, Lee J, Kang B, Lee P, Kwon J, Lee SS, Yang MY (2014) Flexible electronics: fast plasmonic laser nanowelding for a Cu-nanowire percolation network for flexible transparent conductors and stretchable electronics. *Adv Mater* 26:5808–5814
- [28] Tang Y, Gong S, Chen Y, Yap LW, Cheng W (2014) Manufacturable conducting rubber ambers and stretchable conductors from copper nanowire aerogel monoliths. *ACS Nano* 8:5707–5714
- [29] Johnson CJ, Dujardin E, Davis SA, Murphy CJ, Mann S (2002) Growth and form of gold nanorods prepared by seed-mediated, surfactant-directed synthesis. *J Mater Chem* 12:1765–1770
- [30] Zhang SH, Jiang ZY, Xie ZX, Xu X, Huang AR, Zheng LS (2005) Growth of silver nanowires from solutions: a cyclic penta-twinned-crystal growth mechanism. *J Phys Chem B* 109:9416–9421
- [31] Huang X, Zheng N (2009) One-pot, high-yield synthesis of 5-fold twinned Pd nanowires and nanorods. *J Am Chem Soc* 131:4602–4603
- [32] Xu F, Zhu Y (2012) Highly conductive and stretchable silver nanowire conductors. *Adv Mater* 24:5117–5122
- [33] Li W, Zhang H, Gao Y, Jiu J, Li CF, Chen C, Hu D, Goya Y, Wang Y, Koga H (2016) Highly reliable and highly conductive submicron Cu particle patterns fabricated by low temperature heat-welding and subsequent flash light sinter-reinforcement. *J Mater Chem C* 5:1155–1164
- [34] Han S, Hong S, Yeo J, Kim D, Kang B, Yang MY, Ko SH (2015) Nanowires: nanorecycling: monolithic integration of copper and copper oxide nanowire network electrode through selective reversible photothermochemical reduction. *Adv Mater* 27:6397–6403
- [35] Jiu J, Nogi M, Sugahara T, Tokuno T, Araki T, Komoda N, Sugauma K, Uchida H, Shinozaki K (2012) Strongly adhesive and flexible transparent silver nanowire conductive films fabricated with a high-intensity pulsed light technique. *J Mater Chem* 22:23561–23567
- [36] Ding S, Jiu J, Tian Y, Sugahara T, Nagao S, Sugauma K (2015) Fast fabrication of copper nanowire transparent electrodes by a high intensity pulsed light sintering technique in air. *Phys Chem Chem Phys* 17:31110–31116
- [37] Kim HS, Dhage SR, Shim DE, Hahn HT (2009) Intense pulsed light sintering of copper nanoink for printed electronics. *Appl Phys A* 97:791–798
- [38] Zhu Y, Qin Q, Xu F, Fan F, Ding Y, Zhang T, Wiley BJ, Wang ZL (2012) Size effects on elasticity, yielding, and fracture of silver nanowires: in situ experiments. *Phys Rev B Condens Matter* 85:045443
- [39] Jin M, He G, Zhang H, Zeng J, Xie Z, Xia Y (2011) Shape-controlled synthesis of copper nanocrystals in an aqueous solution with glucose as a reducing agent and hexadecylamine as a capping agent. *Angew Chem Int Ed Engl* 123:10560–10564
- [40] Inui T, Koga H, Nogi M, Komoda N, Sugauma K (2015) A miniaturized flexible antenna printed on a high dielectric constant nanopaper composite. *Adv Mater* 27:1112–1116

- [41] Kamyshny A, Magdassi S (2014) Conductive nanomaterials for printed electronics. *Small* 10:3515–3535
- [42] Fujisaki Y, Koga H, Nakajima Y, Nakata M, Tsuji H, Yamamoto T, Kurita T, Nogi M, Shimidzu N (2014) Flexible electronics: transparent nanopaper-based flexible organic thin-film transistor array. *Adv Funct Mater* 24:1656–1656
- [43] Nogi M, Komoda N, Otsuka K, Suganuma K (2013) Foldable nanopaper antennas for origami electronics. *Nanoscale* 5:4395–4399